Front. Earth Sci. 2022, 16(4): 890–905
https://doi.org/10.1007/s11707-022-0965-6

RESEARCH ARTICLE

Comprehensive evaluation of hydrological drought characteristics and their relationship to meteorological droughts in the upper Tarim River Basin, central Asia

Yanyun XIANG[1,2], Yi WANG (✉)[3], Yaning CHEN[2,4], Qifei ZHANG[5], Hongwei LI[2,4]

1 School of Public Administration, Shanxi University of Finance and Economics, Taiyuan 030000, China
2 State Key Laboratory of Desert and Oasis Ecology, Xinjiang Institute of Ecology and Geography, Chinese Academy of Sciences, Urumqi 830011, China
3 School of Water Resources and Hydropower Engineering, North China Electric Power University, Beijing 102206, China
4 University of Chinese Academy of Sciences, Beijing 100049, China
5 School of Geographical Sciences, Shanxi Normal University, Taiyuan 030000, China

Abstract Comprehensive evaluation of the characteristics and mechanisms of droughts is of great significance to drought risk prediction and prevention. The 3-monthly scale Standardized Runoff Index (SRI-3) and 3-monthly scale Standardized Precipitation Evapotranspiration Index (SPEI-3) were employed herein to characterize hydrological and meteorological droughts, respectively, within the four upper subbasins of the Tarim River Basin (TRB) during 1961–2015. The propagation of droughts was also evaluated. The hydrological drought duration (Dd) and drought severity (Ds) were determined by Run theory, and Copula functions were adopted to investigate the hydrological drought probabilities and return periods. The propagation relationships of hydrological and meteorological droughts were assessed. The results indicated that: 1) hydrological drought index (SRI-3) significantly increased in the TRB from 1961 to 2015; the increase was most significant in winter. Meteorological drought index (SPEI-3) exhibited a weak upward trend through time; 2) the characteristics of hydrological droughts varied between the subbasins; increases in the SRI were most significant in the Yarkand and Hotan Rivers, whereas the Dd and Ds of hydrological droughts were higher in the Kaidu and Yarkand Rivers; 3) Frank Copula was the most closely fitted Copula function in the four subbasins of the TRB and yielded average drought return periods of 4.86, 4.78, 3.72, and 5.57 years for the Kaidu, Aksu, Yarkand, and Hotan River Basins, respectively. The return periods in the four subbasins were generally less than 10 years from 1961 to 2015; 4) a cross wavelet transform (XWT) exhibited a significant positive correlation between hydrological and meteorological droughts, except for the Yarkand River Basin, which exhibited a significant negative correlation. Besides, the propagation relationship of meteorological droughts to hydrological droughts showed remarkable seasonal variations.

Keywords hydrological drought, meteorological drought, Copula, drought propagation

1 Introduction

Tarim River, located in the arid area of northwest China, is the largest inland river in the country and serve as an extremely important water resource in Xinjiang Uygur Autonomous Region. Tarim River Basin (TRB) is rich in natural resources and is an important base for grain, cotton and fruit production in China. While drought is one of the most frequent and predominant natural disaster in the TRB since it is characterized by a temperate continental climate with low rainfall, high temperature and strong evaporation (Chen et al., 2016a, 2016b), and extreme drought events also have a serious impact on both the ecological environment and human life in the basin. Thus, drought monitoring and related mechanism research has become one of the most urgent topics for the local development and disaster mitigation in TRB.

According to the American Meteorological Society, drought can be divided into several types, those are, hydrological droughts, meteorological droughts, agricultural droughts and socio-economic droughts. Hydrological drought refers to a shortage of water caused by an

Received May 17, 2021; accepted December 22, 2021

E-mail: hywy02@foxmail.com

imbalance between surface water and groundwater income and expenditure. Its occurrence has important impacts on regional agriculture, ecology and socio-economic development. Climate change is resulting in more frequent, longer lasting, and more serious hydrological droughts than in the past (Williams et al., 2015; Gudmundsson et al., 2021). Meteorological drought usually occurs for the long-term lack of rainfall (Zhou et al., 2021), it can influence river runoff supply and hydrological processes, thereby may generate a hydrological drought. Although meteorological drought and hydrological drought represent two different phenomena, researchers have found that hydrological droughts may generally lag behind meteorological droughts, and drought propagation usually has regional characteristics, for various factors can influence drought propagation, such as human activities, basin characteristics and climate characteristics (Oloruntade et al., 2017; Xu et al., 2019; Gu et al., 2020; Li et al., 2020; Wang et al., 2020b). While, in the TRB, the high temperature may not only cause meteorological drought, but also will accelerate the snow and ice meltwater in the mountainous regions. Subsequently, the generated meltwater may alleviate the problem of low runoff (hydrological drought) caused by a scarcity of precipitation (a meteorological drought) in the region. Therefore, the droughts mechanism and hydrological system of the TRB is an important issue worth in-depth study. However, there are very few systematic researches on hydrological drought and its relationships with meteorological drought under the context of basin hydrological system in the TRB. So, there is a need for a more comprehensive comprehending of the characteristics of droughts and their internal mechanisms of behavior for a better drought analysis and evaluation in the TRB.

Drought monitoring and evaluation usually requires the selection of a drought indicator to characterize different categories of drought. Among various indicators, the Standardized Runoff Index (SRI) has been extensively used in hydrological drought analysis for its simple construction, comparability in time and space as well as simplicity in computation (Shukla and Wood, 2008; Li et al., 2016). And Standardized Precipitation Evapotranspiration Index (SPEI), which considers both evapotranspiration and precipitation, can better characterize meteorological droughts in arid region. Moreover, the drought characteristics can be described by drought variables, including drought frequency, duration, severity, probabilities, and return periods (Dodangeh et al., 2017; Chen et al., 2019b). Independent evaluations of individual drought variable cannot fully characterize drought characteristics, univariate drought variable analysis may lead to overestimation or underestimation of drought risk associated with water management (Mercado et al., 2016; Jiao and Yuan, 2019). Therefore, it is necessary to use joint drought variables to comprehensively analyze and evaluate drought events. Run theory is an important stochastic theoretical approach and it can accurately identify individual drought variable, like duration and severity (Fernández and Salas, 1999). Copula functions are commonly cited in drought characterization analysis (Zhang and Singh, 2007; Serinaldi et al., 2009; Peng et al., 2010; Dodangeh et al., 2017; Bushra et al., 2019; Xiang et al., 2020). They can effectively combine these drought variables and analyze the joint probability distribution and return period of droughts from the perspective of a multivariate association (Kao and Govindaraju, 2010; Mirabbasi et al., 2011).

This study will focus on the evaluation of hydrological droughts characteristics and their relationship to meteorological droughts in the upper Tarim River Basin. In the TRB, most runoff are generated from the mountainous areas, and downstream areas are irrigation area heavily influenced by human activities. Thus, the study of runoff processes in the TRB needs to target the upper part of the basin at the mountain pass. Therefore, this study selected four key upper catchments of the TRB in China for analysis due to the less human disturbance, including the Kaidu River Basin (KRB), Aksu River Basin (ARB), Yarkand River Basin (YRB), and Hotan River Basin (HRB). The investigation characterizes the hydrological and meteorological drought characteristics of the basin based on the SPEI and SRI and their relationships in the four source streams of the TRB were analyzed. The main points in this paper are as follows: (i) to characterize hydrological and meteorological drought of the TRB through the SRI and SPEI; (ii) to determine the drought duration (Dd) and drought severity (Ds) and select the most fit distributions; (iii) to establish the two-dimension joint Copula distributions of hydrological drought and return period analysis; and (iv) to determine the relationship between hydrological and meteorological droughts by wavelet methods. The results of the present research can be used in the evaluation of hydrological drought risk and the prediction of hydrological drought in arid inland basins.

2 Materials

2.1 Study area

The TRB lies in northwest China, surrounded by several high mountains, such as Tian Shan Mountains, Karakoram Mountains, and Pamir Plateau (Fig. 1). The basin covers 1.02 million km^2. Climatically, the TRB is far from the ocean, and is characterized by spatially diverse climatic types, including a temperate continental climate and temperate desert climate. There are 114 headwater subbasins in the TRB that were historically hydraulically connected to the main stream. However, after the 1950s, by reason of natural and anthropogenic effects, the water sources of the Tarim River have been reduced to only the

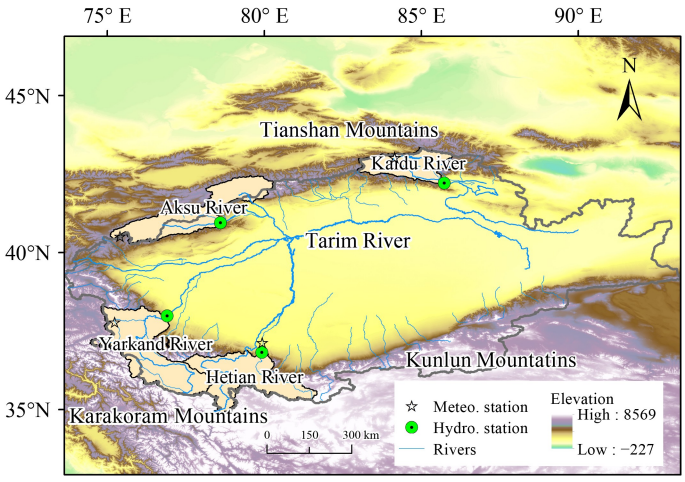

Fig. 1 Location of TRB.

Aksu River, the Hotan River, the Yarkand River, and the Kaidu River, thus forming a drainage pattern consisting of "four sources and one stem" within the TRB (Chen et al., 2006). The water supply of the TRB is mainly from snow and ice meltwater widely distributed in the high mountain zones and precipitation from mid-mountain zones. The production of water in the source area is relatively abundant and provides an important water supply for social and economic development in the basin (Chen et al., 2006; Fang et al., 2018).

The average annual surface runoff in the TRB is 398.3×10^8 m^3. Precipitation in the downstream is scarce and does not produce stream flow. Thus, downstream desert ecosystems and oasis agricultural development all depend on water from the upper reaches. In addition, global warming has drastically altered the hydrological cycle in the TRB in recent decades (Chen et al., 2006, 2016b), meteorological and hydrological events have occurred frequently. Runoff within the TRB is mainly produced by glacial meltwater in the high mountainous areas, and the distribution is very uneven during the year. Hydrological drought has an obvious impact on hydrology and ecology in the basin, especially during spring (March to May), droughts pose a serious threat to agricultural and ecological water use.

2.2 Data sets

In this paper, monthly runoff data from the mountain outlet at four hydrological stations during the period 1961–2015 in the four subbasins of the TRB were obtained from the Xinjiang TRB Management Bureau, which represent the input runoff to those subbasins.

As for the meteorological data, considering there is only one meteorological station in each of the four watersheds and the underlying surface and elevation within the basin area are different, so, it is difficult to represent the climate change characteristics within the basin. Therefore, the monthly gridded meteorological data from the Climatic Research Unit (CRU) data between 1961 and 2015 were used in this study, and the CRU data are gridded to 0.5×0.5-degree resolution, based on analysis of over 4000 individual weather station records all over the world, and shows good correlations with station observed data in Tarim River Basin (Wang et al., 2020a). Specifically, the average value of CRU data above the mountain outlet of the whole basin were calculated and used. The data included precipitation, temperature and potential evapotranspiration, which were used to calculate the SPEI.

2.3 Methods

2.3.1 Standard Precipitation and Evapotranspiration Index (SPEI)

SPEI (Vicente-Serrano et al., 2020), utilized herein, is an indicator commonly used for quantification and monitoring of meteorological droughts. The SPEI was based on the difference between precipitation (P) and potential evapotranspiration (PET). These data were extracted from the CRU data set. A detailed description of their calculation follows.

First, calculate the difference between monthly P and PET:

$$D_m = P_m - ET_{0m}, \tag{1}$$

where m is the number of months, P_m represents monthly precipitation, and ET_{0m} represents PET.

Then, D_m was aggregated and normalized according to different time scales:

$$\begin{cases} D^i_{m,n} = \sum_{j=13-i+n}^{12} D_{m-1} + \sum_{j=1}^{n} D_{m,j}, & n < i \\ D^i_{m,n} = \sum_{j=n-i+1}^{n} D_{m,j,n}, & n \geqslant i, \end{cases} \tag{2}$$

where i is the timescale (months) of the aggregation and n is the calculated month.

The Log-Logistic (Log-L) distribution is applied to fit the aggregated differences between P and PET (Trenberth and Fasullo, 2013). Once determined, $F(D)$ can be calculated

$$F(D)=\left[1+\left(\frac{\alpha}{D-\gamma}\right)^{\beta}\right]^{-1}, \tag{3}$$

where α, β, and γ are the scale, shape and position parameters of the Log-L distribution, respectively.

Finally, SPEI can be calculated

$$\mathrm{SPEI}=W-\frac{c_1+c_2W+c_3W^2}{1+t_1+t_2W^2+t_3W^3}, \tag{4}$$

and

$$\begin{cases} W=\sqrt{-2\ln P}, & P\leqslant 0.5 \\ W=\sqrt{-2\ln(1-P)}, & P>0.5 \end{cases}, \tag{5}$$

where P means the probability of exceeding a determined D value and is given as $P=1-F(D)$ and $c_1=2.515517$, $c_2=0.802853$, $c_3=0.010328$, $t_1=1.432788$, $t_2=0.189269$, $t_3=0.001308$ (Ayantobo et al., 2018; Tirivarombo et al., 2018).

2.3.2 Standard Runoff Index (SRI)

SRI (Vicente-Serrano et al., 2020; Tak and Keshari, 2020), utilized herein, is an indicator commonly used for quantification and monitoring of hydrological droughts. The computation procedure of SRI is similar to that of the SPEI, however, unlike SPEI, there is no universally recommended probability distribution for the calculation of SRI due to the influence of climate, anthropogenic factors, and geography on runoff (Svensson et al., 2017). Therefore, it is necessary to examine the probability distribution of runoff and select the optimal distribution function to calculate the SRI (Telesca et al., 2012; Bloomfield and Marchant, 2013). The seven distribution functions (Table 1) were first fitted by the maximum likelihood method. Subsequently, the goodness-of-fit of these distributions were tested by the Chi-square test to assess the fitting results between the distribution and the runoff data, the most appropriate fitting function was selected on the principle of the maximizing statistic p value calculated by Chi-square test (Vicente-Serrano et al., 2012). SRI can be calculated after selecting the optimal distribution function of runoff through converting the cumulative probability to a standard normal distribution.

Both SRI and SPEI have a characteristic of multiple time scales, which reflect different hydrological drought phenomena, a 3-month scale SRI (SRI-3) and SPEI (SPEI-3) was chose in this paper to characterize hydrological droughts.

Table 1 Seven distribution functions and parameters

Functions	Formula	Parameters
Pearson Type III (P-II1)	$f(x)=\frac{1}{\alpha\Gamma(\beta)}\int_{\gamma}^{x}\left(\frac{x-\gamma}{\alpha}\right)^{\beta-1}e^{-\left(\frac{x-\gamma}{\alpha}\right)}$	α, β, γ
Weibull (WBL)	$f(x)=1-\exp\left(-\left(\frac{x-\gamma}{\beta}\right)^{\alpha}\right)$	α, β, γ
Log-Logistic (Log-L)	$f(x)=\left[1+\left(\frac{\beta}{x-\gamma}\right)^{\alpha}\right]^{-1}$	α, β, γ
Gamma (GM)	$f(x)=\frac{1}{b^{a}\Gamma(\mathrm{a})}x^{a-1}e^{\frac{-x}{b}}$	a, b
Gen. Extreme Value (GEV)	$f(x)=\exp(-\exp(k^{-1}\ln(1-\frac{k(x-\mu)}{\sigma})))$	k, σ, μ
Log-Normal (LN)	$f(x)=\frac{1}{x\sigma\sqrt{2\pi}}\exp\left\{\frac{-(\ln x-\mu)^2}{2\sigma^2}\right\}$	σ, μ
Gen. Pareto (GP)	$f(x)=1-\left[1-\frac{k}{\alpha}(x-\epsilon)\right]^{1/k}$	k, α, ε

2.3.3 Run theory

In this study, run theory was adopted to determine hydrological drought variables based on the calculated SRI (Wu et al., 2019). Here, two hydrological drought characterizes variables drought duration (Dd) and drought severity (Ds) were selected, then, drought characteristics and probabilities of the hydrological and meteorological droughts can be investigated. When the SRI values were below the threshold X_0, the corresponding time was identified as a drought event. Dd represents the duration of a drought event, the count of continuous months at which the value of the SRI is below the threshold X_0, referring to previous studies, a threshold X_0 of −0.5 was used to identify a drought event (Xiang et al., 2020). Ds means the severity of a hydrological or meteorological drought event, is the absolute sum of all SRIs value during a drought event. Using the above definitions, hydrological drought identification was carried out by calculating the SRI over a 3-month scale (SRI-3).

2.3.4 Copula models

After determining the Dd and Ds, Copula models were applied to fit the two variables. The marginal distribution for Dd and Ds were first established, and the dependence between the two variables should be examined using the Kendall rank, Spearman's rank-order, and Pearson product-moment correlation coefficients. Twenty marginal distribution functions (e.g., GP, GM, GEV) on Dd and Ds were fit to the data. The optimal marginal distribution functions were selected based on K-S and Akaike Information Criterion (AIC) methods. The best fit distribution function was determined as the type of marginal distribution for the drought characteristic variables, provided that it passed the significance test. Then, a two-dimensional Copula function was used to construct a 2D Copula which was fit to the joint distribution functions of the two indicators (Dd and Ds). Commonly used two-dimensional symmetric Archimedean Copula functions,

Table 2 Two-dimensional Archimedean Copula functions

Copula functions	Formula and parameter
Gumbel Copula	$C(Dd,Ds)=\exp\left\{-\left[(-\ln Dd)^{\theta}+(-\ln Ds)^{\theta}\right]^{1/\theta}\right\},\ \theta\geqslant 1$
Clayton Copula	$C(Dd,Ds)=\left(Dd^{-\theta}+Ds^{-\theta}-1\right)^{-1/\theta}$
Frank Copulaa	$C(Dd,Ds)=-\frac{1}{\theta}\ln\left[1+\frac{\left(e^{-\theta Dd}-1\right)\left(e^{-\theta Ds}-1\right)}{e^{-\theta}-1}\right]$

including Clayton Copula, Frank Copula and Gumbel Copula (Table 2), were applied. The parameters of the functions were calculated by maximum likelihood estimation method. The goodness of fit (GOF) of the Copula functions was tested by means of the Root Mean Square Error (RMSE) and Nash-Sutcliffe Efficiency coefficient (NSE). The most suitable functions were then selected on the principle of minimizing the RMSE and maximizing the NSE. The optimal copula functions were finally established in the four upper subbasins of the TRB.

The joint return period represents the reoccurrence interval of a drought events (Wu et al., 2019), which means the return period when at least one hydrological drought variables exceed a certain value. After establishing two-dimensional joint Copula functions of Dd and Ds, the return periods of hydrological droughts can be calculated. Detailed formulas can be referred to Xiang et al. (2020).

The approach assumes that X_1 and X_2 represent the sequence of characteristic variables with dependent relationships to drought events. The marginal distribution functions were $u_1 = F(x_1)$, $u_2 = F(x_2)$. The two-dimensional joint return period can be expressed as

$$T=\frac{N}{n\times P(X_1\geqslant x_1\cup X_2\geqslant x_2)}=\frac{N}{n\times(1-C(u_1,u_2))}, \quad (6)$$

where T represents the joint return period of the drought elements, N is the length of the time series of drought analysis, and n is the number of times of drought occurrence, and $C(F_{x_1}(x_1),F_{x_2}(x_2))$ represents the joint probability of a two-dimensional variable group.

2.3.5 Mann-Kendall (M-K) trend test

Trend test is a significant element of temporal analysis in the fields of climate research and hydrology. A range of statistical methods are used to assess changes in time series trends (Hamed and Ramachandra Rao, 1998). These methods are mainly divided into two categories: parametric and nonparametric. Climate and hydrological time series often possess non-normal distributions and contain missing values. Therefore, changes in trends identified by parametric statistical tests are typically not credible (Hirsch and Slack, 1984). Nonparametric tests are not limited by assumptions of normality or missing data, making them more effective. The M-K trend test method is a representative nonparametric test, which is also commonly used to evaluate hydro-meteorological time series.

For a time series x, the statistic S of Mann-Kendall trend test is as follows:

$$S=\sum_{i=1}^{n-1}\sum_{j=i+1}^{n}\operatorname{sgn}(x_j-x_i), \quad (7)$$

where x_i, x_j represent the sequential data values of the time series x, n is the length of time series, $\operatorname{sgn}(x_j-x_i)$ is an indicator function that takes on the values 1, 0, or −1.

In this paper, Z_s values were employed to characterize the variation trends, $Z_s > 0$ indicates a downward drought trend, and $Z_s < 0$ indicates an upward drought trend. Z_s can be calculated

$$\begin{cases} Z_s=\dfrac{S+1}{\sqrt{n(n-1)(2n+5)}}, & S>0 \\ Z_s=0, & S=0 \\ Z_s=\dfrac{S+1}{\sqrt{n(n-1)(2n+5)}}, & S<0 \end{cases}. \quad (8)$$

In a two-sided test for the trend, the null hypothesis of no trend is rejected if $|Z_s|\geqslant Z_{s(1-\alpha/2)}$, where α is the significance level. The trend is said to be significant increasing if Z is positive and the absolute value is greater than the level of significance, or it is decreasing if Z_s is positive and greater than the level of significance.

2.3.6 Wavelet analysis

The link between meteorological drought and hydrological drought was usually analyzed by Cross wavelet transform (XWT) (Torrence and Compo, 1998) and wavelet coherence (WTC) (Torrence and Webster, 1999) between monthly SRI and SPEI (SRI-1 and SPEI-1) (Huang et al., 2017; Ma et al., 2019; Zhong et al., 2020). XWT can explore the relationship between two time series in high power regions, in contrast, WTC can describe the relationship between two time series in low power regions, and can also be used to measure the correlation between two time series in the time and frequency domain space. The correlation between the two sequences in the wavelet coherence spectrum may be significant even if it corresponds to a low energy region in the cross-wavelet power spectrum (Wang et al., 2020b).

2.3.7 Correlation analysis

The propagation characteristics and time from meteorological drought to hydrological drought was explored base on correlation analysis in this study. The analysis the propagation time was based on SPEI data that were used to characterizes different types of droughts on multiple time scales. The correlation between the SPEI and the corresponding SRI values was then determined. The correlation was conducted using a 1-month time scale for

SPEI and time scales ranging from 1 to 24 month for SRI. In this paper, the Pearson correlation coefficient was chosen to characterize the correlation between the SPEI and SRI.

3 Results

3.1 GOF test of runoff distributions

The most fitted probability distributions for the monthly runoff series (1961－2015) from the four hydrological stations were determined by use of the K-S test at a 5% significance level (P-value = 0.05). As shown in Fig. 2, the seven distributions exhibited a suitable fit to the streamflow data because most of the P-values exceeded the critical value of P-value (0.05). The GP, GEV, GM, and GP distributions were the most suited for the KRB, ARB, YRB, and HRB, respectively, since the P-value for those distributions are higher than other distributions. Hence, they can be applied for SRI computations in the four basins.

3.2 Hydrological drought characteristics

The hydrological drought index (SRI) of the four subbasins during the period 1961－2015 were calculated using the four best fitted distributions identified in the previous section. Figure 3 shows the trend of hydrological droughts index on a 3-monthly scale (SRI-3) in the four upper subbasins of the TRB. The results show that all four basins exhibited an increase in SRI from 1961 to 2015. In addition, the predominance of positive and negative values throughout the time period shows that SRI values calculated for all four basins changed from negative to more positive values in the 1990s, i.e., droughts dominated the study area before 1990, and the basins became wetter thereafter. However, the degree of increase differs among the four subbasins, with the YRB and HRB showing the most significant upward trend and greater interannual fluctuations.

To further understand temporal changes in SRI and their significant characteristics in each subbasin by month, season and year, the M-K trend test was carried out for SRI at each time scale. The trend in the Z_s values of the SRI changed as a function of the observational period (i.e., by month, season and year) (Fig. 4). The SRI in all four subbasins increased at different rates and times depending the time scales. On the monthly scale, SRI in each subbasin increased mostly from January to March and from October to December, reaching a significance level of 95%, while the changes in SRI from June to August did not reach a statistically significant level. On the seasonal scale, SRI increased most significantly in winter (December to February, DJF), with Z_s values of 3.19, 4.36, 5.79, and 7.03 in the KRB, ARB, YRB, and HRB, respectively. The magnitude of change was less significant in autumn (September to November, SON) and spring (March to May, MAM), but changes in SRI during these two seasons also reached the 95% significance level. In summer (June to August, JJA), the trend in the Z_s values failed to reach the 95% significance level, indicating that SRI values did not significantly increase. Comparing the multi-year SRI trends in each basin, the YRB and HRB showed the most significant trends both on monthly and seasonal scales and on annual scales, followed by the ARB.

3.3 Hydrological drought probability and return period

3.3.1 Characteristics of hydrological drought variables

To better understand the characteristics of hydrological

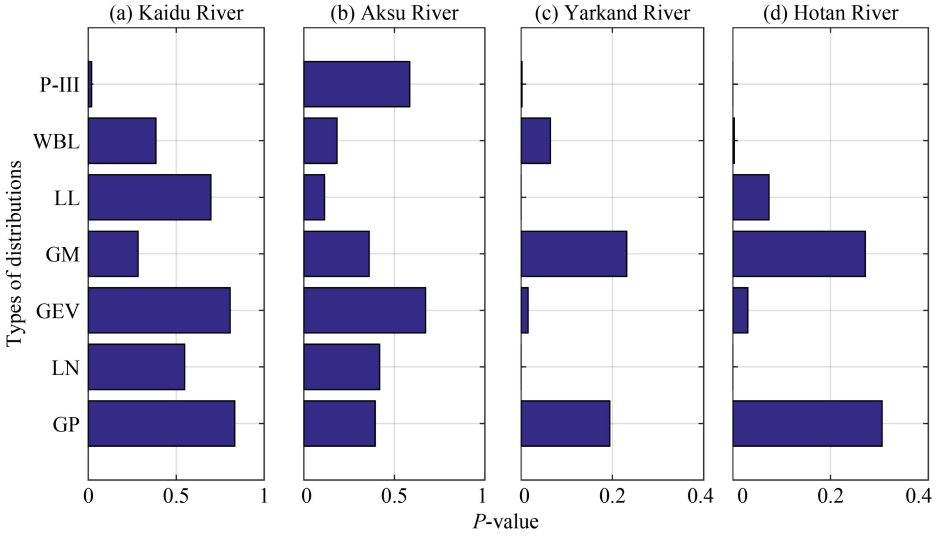

Fig. 2 P-values for the different types of distributions fitting monthly runoff data.

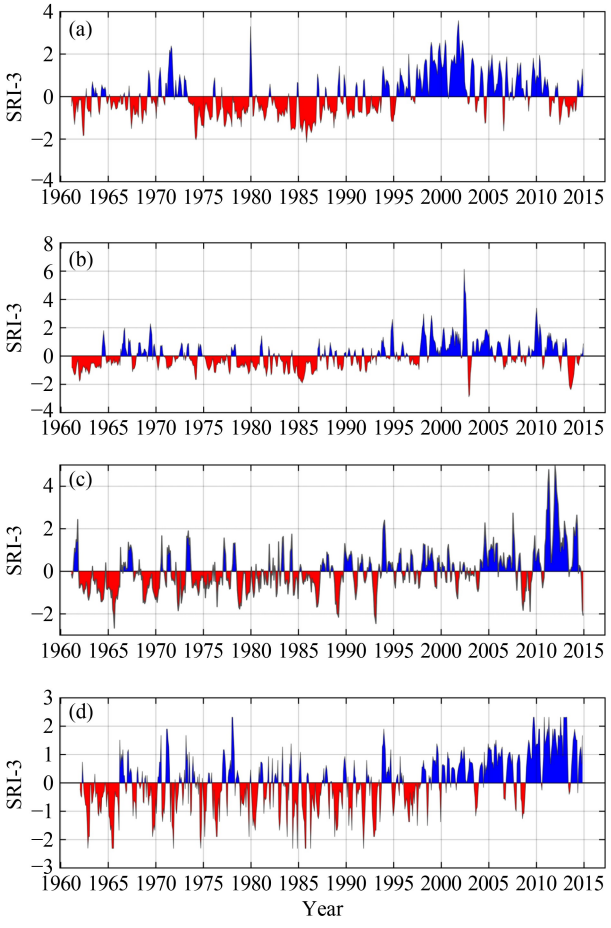

Fig. 3 Time series of SRI-3 from 1961 to 2015 of (a) KRB, (b) ARB, (c) YRB, and (d) HRB.

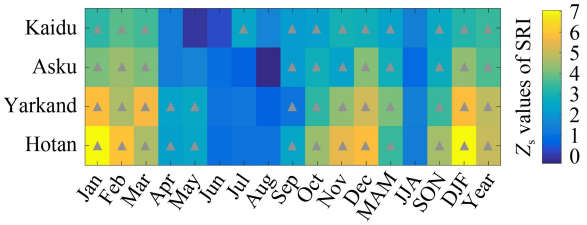

Fig. 4 Z_s values of SRI in the four basins during 1961–2015. The gray triangle means the variation trend reached the 95% significance level.

drought events, Dd and Ds for hydrological droughts in each basin were calculated using Run theory. The distribution of Dd and Ds were then plotted on by violin plots. The black circles in Fig. 5 indicate the median value of Dd and Ds from 1961 to 2015, and the thick orange bar in the center represents the interquartile range of value. Comparing the median values and interquartile ranges of four subbasins, the hydrological Dd and Ds in the YRB and HRB were higher than the KRB and ARB between 1961 and 2015. On each side of the gray line is a kernel density estimation to show the distribution shape of the data, wider sections of the violin plot represent a higher probability that Dd or Ds will reach to the given value, the skinnier sections represent a lower probability. The hydrological Dd are more widely distributed than Ds, these wide patterns are mainly due to the long duration of droughts, and imply great diversities across drought duration. Besides, the trends in Z_s values of hydrological Dd and Ds were analyzed using the MK trend test. Results show that Z_s of Dd was greater than zero in all the subbasins except the YRB (Z_s = 0.37, 0.07, −0.05, 0.40, respectively), while the hydrological Z_s of Ds was greater than zero only in the HRB (Z_s = −0.82, −0.97, −0.12, 0.52, respectively). Z_s of Ds was less than zero in the other basins, it shows that the hydrological drought events in the TRB develop to longer duration and lower drought intensity.

3.3.2 Copula models and return periods

In this study, the most suitable marginal distribution of the two variables was initially selected based on a Bayesian Information Criterion (BIC) GOF tests. The GOF analysis showed that the marginal distribution functions of Dd and Ds for all four subbasins exhibited a GP distribution (Table 3). The correlation between the four groups of variables in the four subbasins was also verified; there was a significant correlation between Dd and Ds in each subbasin ($p < 0.05$), indicating that the two variables were highly correlated with each other. The Copula functions could be applied to establish joint distributions to characterize the hydrological droughts of the four studied subbasins.

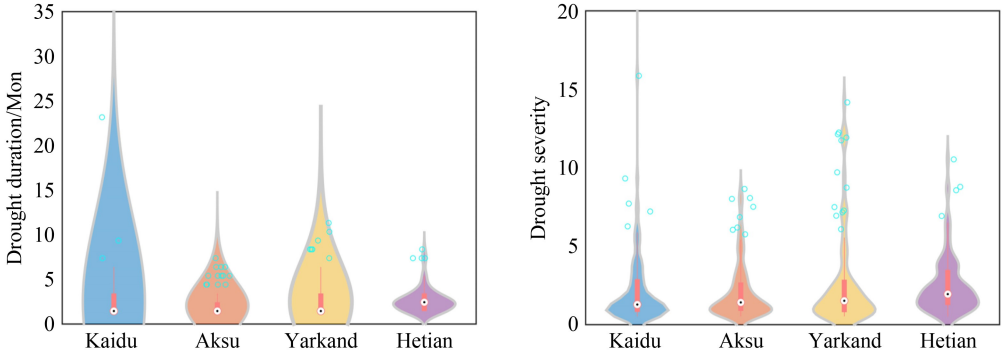

Fig. 5 Violin plot of the hydrological Dd and Ds.

Table 3 Fitted marginal distribution function and correlation coefficient

Basin	Drought characteristics	Fitted distribution	Parameters			Kendall rank	Spearman's rank-order	Pearson product-moment
			k	Sigma	Theta			
KRB	Dd	GP	23.41	0.00	2.00	0.72	0.85	0.97
	Ds	GP	0.34	2.23	1.21			
ARB	Dd	GP	19.84	0.00	2.00	0.66	0.79	0.86
	Ds	GP	−0.32	3.19	1.26			
YRB	Dd	GP	24.33	0.00	2.00	0.82	0.92	0.96
	Ds	GP	0.02	3.57	1.53			
HRB	Dd	GP	15.53	0.00	2.00	0.67	0.79	0.91
	Ds	GP	−0.05	2.16	1.12			

Table 4 Parameters and GOF test results of Copula functions in the four basins

Basin	Clayton			Frank			Gumbel		
	Parameter	RMSE	NSE	Parameter	RMSE	NSE	Parameter	RMSE	NSE
Kaidu	0.06	0.94	0.70	**5.27**	0.75	0.81	1.75	0.75	0.81
Aksu	0.07	1.23	0.56	**3.95**	1.07	0.67	1.58	1.08	0.66
Yarkand	0.06	1.01	0.68	**5.10**	0.77	0.81	1.75	0.77	0.81
Hotan	0.07	1.87	0.26	**4.48**	1.63	0.43	1.67	1.66	0.41

[a] The bold letters mean the best fit Copula function.

Table 4 shows the parameters and the corresponding GOF test parameters of the two-dimensional joint Copula correlation in each subbasin based on Dd and Ds values. The optimal Copula functions was selected as the joint distribution function of Dd and Ds for the four source streams in the TRB based on the principle that the smaller the RMSE and the larger the NSE value, the higher the GOF of copula function. Table 4 showed that the Frank Copula function was the most suitable function to describe Dd and Ds for the KRB, ARB, YRB and HRB. Thus, the Frank Copula was determined the most fit two-dimensional Copula function in the upper TRB.

Based on the GOF test parameters, the joint probability and return periods for the four subbasins from the two-dimensional Copula functions were calculated. The number of hydrological drought events determined was 39, 45, 39, and 62 for the KRB, ARB, YRB, and HRB between 1961 and 2015, respectively. The longest drought durations in the four subbasins were 23 months, 7 months, 11 months, and 8 months, respectively. The maximum Ds reached 37.88, 8.64, 14.16, and 10.53 in the four subbasins, respectively, corresponding to joint return periods of 69.86 years, 80.57 years, 25.08 years, and 110.93 years, respectively. The longest Dd corresponded to the maximum Ds and are always occurred in the same drought event in each basin. The average Dd was 3.95 months, 3.13 months, 4.08 months, and 2.81 months, and the average Ds was 4.69, 3.63, 4.79, and 3.17 within the KRB, ARB, YRB, and HRB, respectively. The average Ds reached a peak value (4.79) in the YRB and a least value (3.17) in the HRB, a difference of only 1.62.

The average joint hydrological drought probabilities for drought events of the KRB, ARB, YRB, and HRB during 1961–2015 were 0.46, 0.46, 0.48, and 0.49, respectively, and the average joint return periods of drought events were 4.86 years, 4.78 years, 3.72 years, and 5.57 years, respectively. The increase in Dd and Ds corresponded to increased drought return periods, and drought events tended to be serious. In summary, the combination of Run Theory and Copula function analysis was able to effectively portray the drought characteristics of the TRB. The frequency of hydrological droughts in the four subbasins was high, and the return periods were generally less than 10 years (Fig. 6).

3.4 The relationship between hydrological and meteorological droughts

This section explores the relationship between hydrological droughts and meteorological droughts in the TRB. First, the SPEI of the four subbasins during the period 1961–2015 were calculated (Fig. 7). All four subbasins exhibited alternating positive and negative values of SPEI throughout 1961–2015. Overall, the KRB and ARB exhibited a weak upward trend in SPEI through time; rates of increase were 0.08/decade and 0.04/decade, respectively. The YRB and HRB exhibited a weak decreasing trend; rates of decrease were 0.06/decade and 0.05/decade, respectively. Furthermore, the changes in SPEI and SRI trends were compared (Fig. 3). It can be seen that the temporal changes in SPEI were less significant compared with SRI, and meteorological droughts have a higher frequency and shorter duration.

Moreover, to further analysis the relationships between

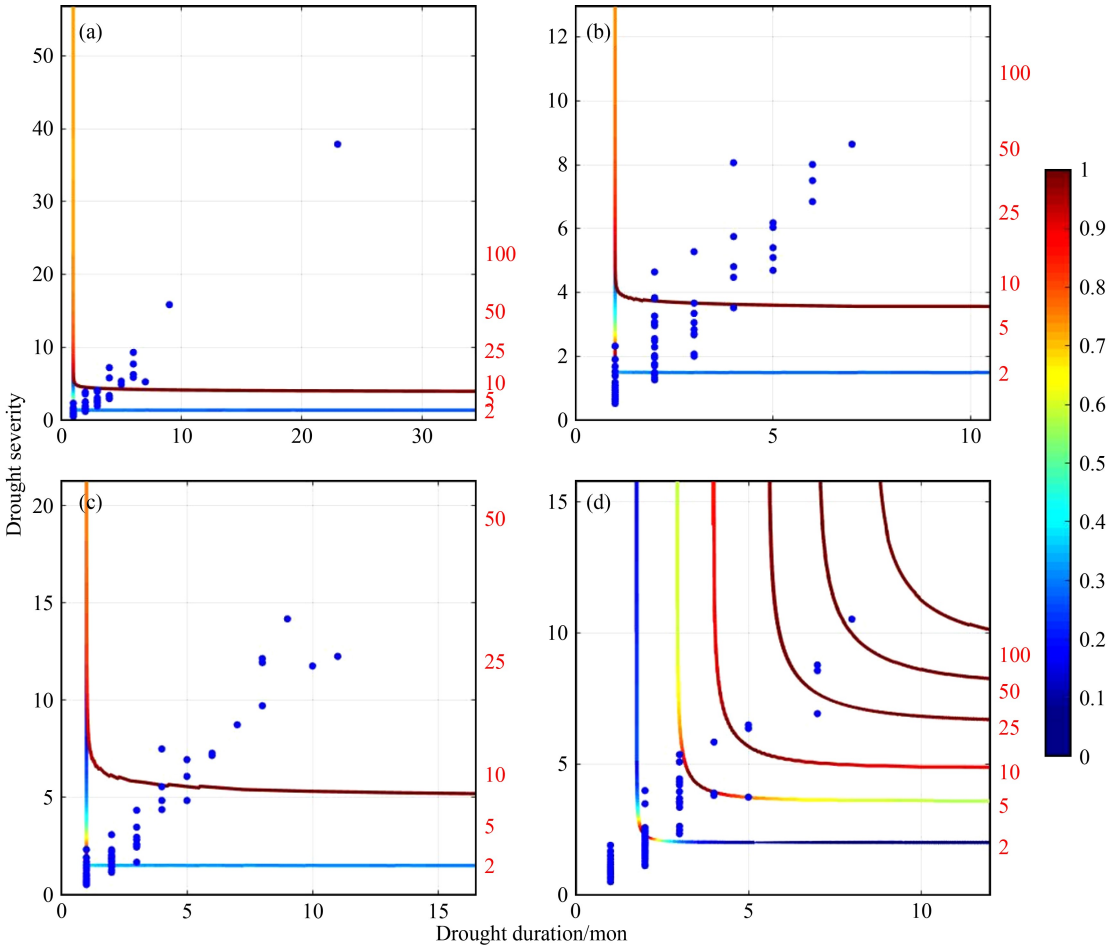

Fig. 6 Drought return period of drought events in (a) KRB, (b) ARB, (c) YRB, and (d) HRB. Blue dots mean hydrological drought events.

meteorological and hydrological droughts in TRB, XWT were applied and the cross-wavelet power spectrum of the monthly SRI and SPEI series from 1961 to 2015 were obtained and shown in Fig. 8. There are two significant resonance cycles of SRI and SPEI in the KRB at the 95% confidence level. These include the 10−14-month signal between 2004 and 2007 and the 6−8-month signal between 2009 and 2011 (Fig. 8(a)). It shows two significant resonance cycles of SRI and SPEI in the ARB at the 95% confidence level, which include the 64–80-month signal between 1982 and 2000 and 7–20-month signal between 1995 and 2004. While there are two significant long-term intermittent oscillation periods between SRI and SPEI in the YRB at a 95% confidence level, which include the 30–40-month signal between 1968 and 1973 and the 64–130-month signal between 1998 and 2005. It also exhibits 2 significant resonance cycles at the 95% confidence level in the HRB, including the 60–64-month signal between 1973 and 1985 and the 102–128-month signal between 1998 and 2002. The phase arrows mostly point right except for YRB, indicating that meteorological drought and hydrological drought presented a significant positive correlation. Notably, the phase arrows in these four subbasins are almost different, indicating that there was heterogeneity in correlation between meteorological drought and hydrological drought.

Figure 9 reveals the features and a 95% confidence level correlation of the SRI and SPEI series in the low power region. Consistent with the result from XWT, at a 95% confidence level, among the four source streams to the TRB, the SRI and SPEI in all subbasins have significant positive correlations, except the YRB. YRB has a significant negative correlation. Summarily, the XWT power spectrum and WTC performance can effectively determine the relationship and detailed characteristics of the oscillation cycles of hydrological droughts and meteorological droughts over time in the four subbasins of the TRB. A positive correlation between hydrological droughts and meteorological droughts indicates that meteorological droughts can lead to the occurrence of hydrological droughts, and the occurrence of hydrological droughts lag meteorological droughts.

3.5 Propagation characteristics of meteorological to hydrological droughts

To analyze the propagation relationship between the two

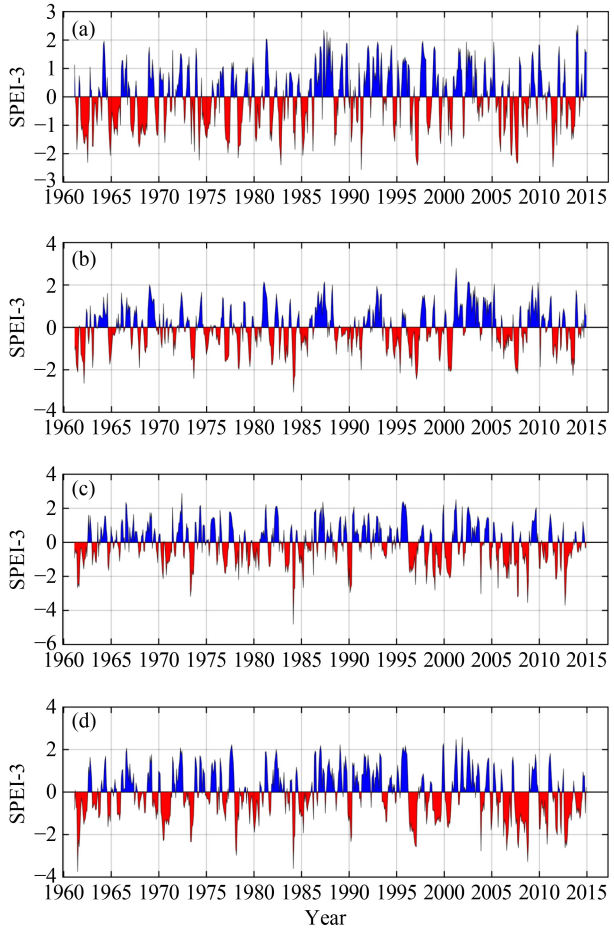

Fig. 7 Time series of SPEI-3 from 1961 to 2015 of (a) KRB, (b) ARB, (c) YRB, and (d) HRB.

kinds of drought events in the four source streams of the TRB, SPEI was calculated for multiple time scales. The time-scale dependent SPEI values are assumed to represent different types of droughts. The correlation between the SPEI values and SRI values was calculated using a range of SPEI time scales varying between 1 and 24 months and an SRI time scale corresponding to 1-month (SRI-1). The steps used to determine the propagation time of meteorological droughts to hydrological droughts are as follows (using the propagation time of a July drought in the KRB as an example). 1) calculate the SPEI values for each of the 1–24-month time scales in July; 2) calculate the SRI-1 values in July; 3) calculate the correlation coefficient between the SPEI of each of the 1–24-month time scales in July to the SRI-1 in July; and 4) given the obtained correlation coefficients, the SPEI time scale with the highest correlation coefficient is the propagation time of July, and the SPEI-2 has the highest correlation with SRI-1 in this example; therefore, the propagation time in July in the KRB is 2 months. 5) The propagation time of drought during a given season is obtained by applying the above-mentioned method using an average propagation time of 3 months from the same season. For example, the drought propagation time in summer is the average value of the drought propagation time in June, July, and August. In accordance with this method, the correlation coefficients between the SPEI-1 to SPEI-24 values and the SRI-1 were calculated for the four study subbasins (Fig. 10). The maximum correlation coefficients between SPEI and SRI at different time scales ($P < 0.01$) can be employed to estimate the propagation time of meteorological droughts to hydrological droughts.

The calculation result is shown in Fig. 10, it can be seen that the propagation relationship between meteorological droughts and hydrological droughts in each subbasin has a specific seasonality and periodicity. The correlation coefficients of SPEI and the 1-month SRI values for each cumulative 24-month period are highest in the KRB and lowest in the HRB. The maximum values of the correlation coefficients in the KRB, ARB, YRB, and HRB are 0.52, 0.47, 0.25, and 0.21, respectively. Taking the KRB as an example, the propagation time of meteorological drought to hydrological drought from January to December was 22 months, 2 months, 9 months, 11 months, 11 months, 3 months, 2 months, 2 months, 2 months, 4 months, 17 months, and 18 months, respectively, and the correlation coefficients were 0.39, 0.29, 0.18, 0.35, 0.52, 0.51, 0.43, 0.38, 0.39, 0.35, 0.25, and 0.28, respectively. In general, the propagation time from meteorological droughts to hydrological droughts showed remarkable seasonal variations, that is, longer in winter and spring (generally greater than 12 months), but shorter in summer and autumn (generally within 12 months).

It's worth noting that the correlation coefficients between SRI-1 and SPEI in these four subbasins are lower than other basins, for example, the basins in humid and semi-humid area. The correlation coefficients between SPEI and SRI in the YRB and HRB are also negative in some months, such as August and October. This differs from the results of Li et al. (2020) on the Shiyang River, as well as the results of Wang (2020b) on the relationships between meteorological droughts and hydrological droughts before conversion in the Yellow River. This difference indicates that the relationship between meteorological droughts and hydrological droughts in the TRB has some unique characteristics; there are no significant negative or positive relationships between those two types of droughts in the TRB, which is likely to be due to the nature of runoff from each source stream to the TRB (i.e., not only are streams recharged by precipitation, but also by glacial and snowmelt, especially in the Karakorum and Kunlun Mountains in the headstream of the YRB and HRB). The combined runoff from precipitation as well as glacier- and snowmelt makes the relationship between meteorological droughts and hydrological droughts more complicated because the occurrence of hydrological droughts is not only affected

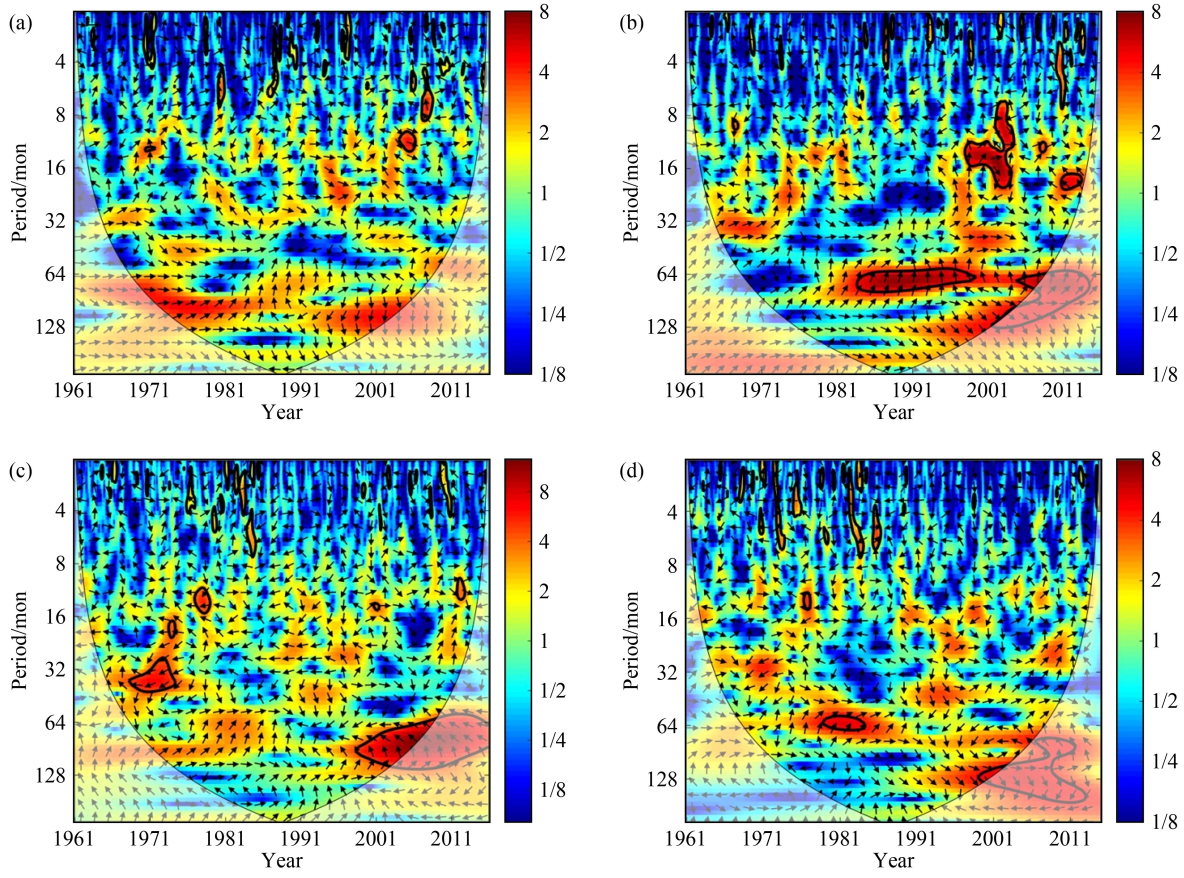

Fig. 8 XWT between the monthly SRI and SPEI sequences at the 95% confidence level from 1961 to 2015 in (a) KRB, (b) ARB, (c) YRB, and (d) HRB. The relative phase relationship is represented as arrows (left-pointing arrows mean negative correlations, and right-pointing arrows mean positive correlations). The color bar represents the wavelet power.

by precipitation, but also by temperature and the storage of glacier ice and snow.

4 Discussion

Comparing the hydrological drought characteristics of the four subbasins in TRB reveals that there are large spatial hydrological differences between them. First, the HRB and YRB have the most significant annual- and seasonal-scale variations in SRI, whereas the KRB has the least significant variation. This lead to differences in the variation of hydrological Dd, Ds and hydrological drought probability in each basin; the differences among the four subbasins are also reflected in the propagation characteristics between hydrological and meteorological droughts. Via correlation analysis of 1–24-month SPEI time scale and 1-month SRI time scale, we found that the correlation coefficients between SPEI and SRI in these four subbasins were low. The SPEI values in the KRB and ARB were positively correlated with SRI, but the correlation between the YRB and HRB was negatively correlated in some months, such as August and October. Hydrological and meteorological droughts are therefore not perfectly aligned, it further reveals that hydrological droughts occurring more frequently are due not only to less rainfall but also to more reasons affecting water condition in the basin. In the basins where snow and ice meltwater accounting a relatively large portion of the river water, such as in the YRB and HRB, the accelerated melting of glacial ice and snow caused by rising temperatures have much greater impact on runoff than increased precipitation (Zhang et al., 2012; Kan et al., 2018).

There are a variety of factors that impact the development of hydrological droughts in the TRB. Most are natural factors, e.g., temperature, precipitation, evaporation, and snow/glacier. Here, we chose four main factors, including annual temperature (Tem), precipitation (Pre), potential evapotranspiration (Pet) extracted from the CRU data set, and annual snow depth, to estimate the relative effects of natural factors on the links between meteorological and hydrological drought factors. As shown in Fig. 11, runoff in those four basins was more correlated with temperature than with precipitation, this is also consistent with the conclusion of Lyu et al. (2015), that is, the runoff of TRB is most affected by temperature change. Snow depth was negatively correlated to runoff

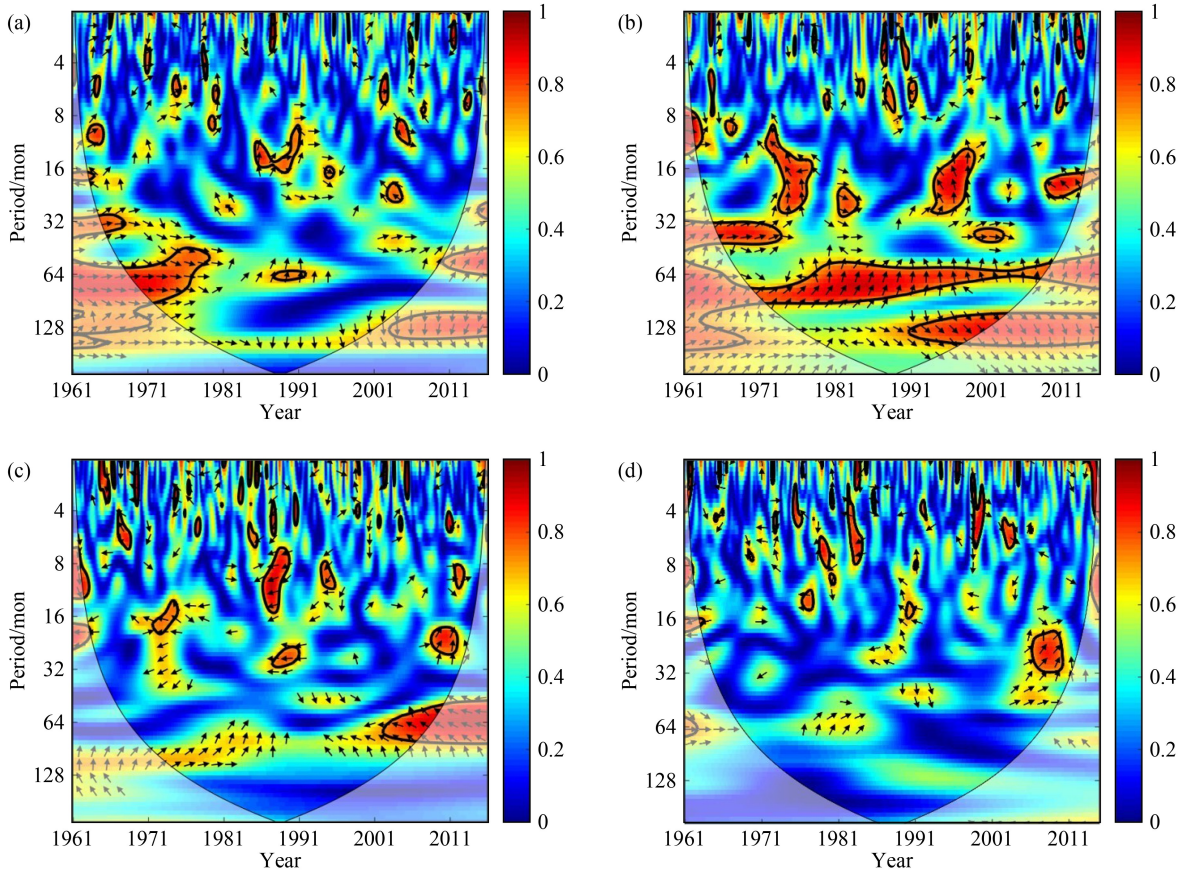

Fig. 9 WTC between the monthly SRI and SPEI series from 1961 to 2015 in (a) KRB, (b) ARB, (c) YRB, and (d) HRB.

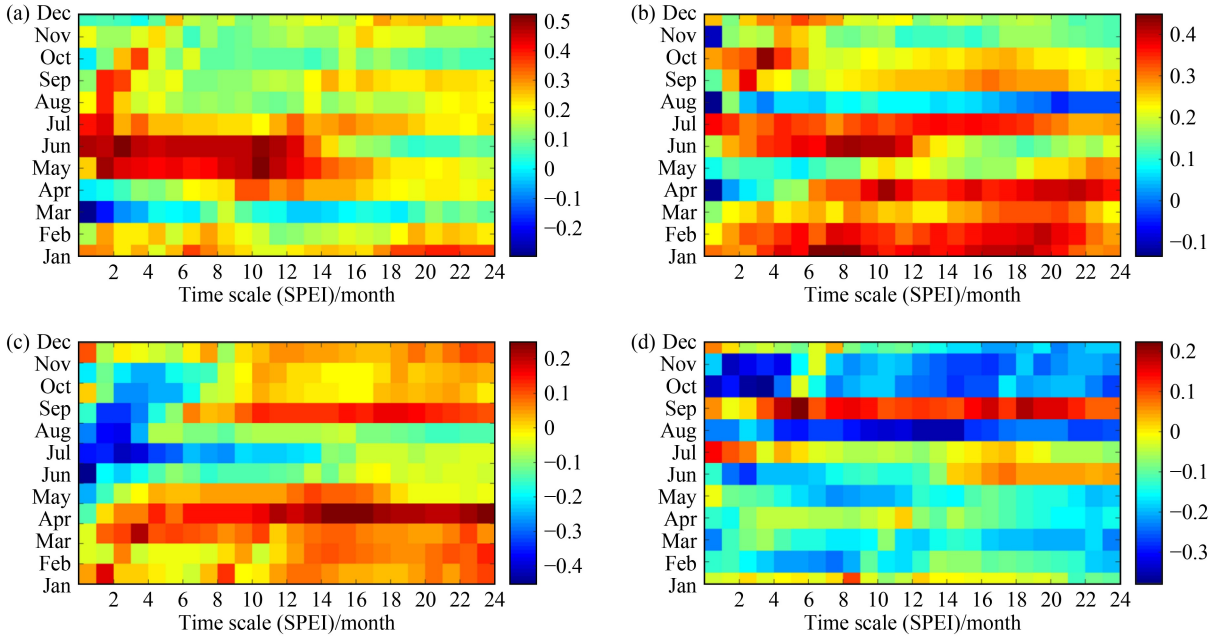

Fig. 10 The correlation coefficients between SPEI of each of the 1–24-month time scales and the SRI-1 in (a) KRB, (b) ARB, (c) YRB, and (d) HRB. The color bars indicate the correlation coefficients. The *x*-axis indicates the SPEI values over the 1 to 24-month time scales, whereas the *y*-axis indicates different months.

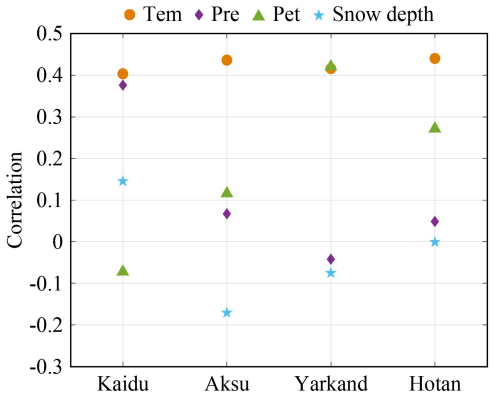

Fig. 11 Correlation between runoff and temperature (Tem), precipitation (Pre), potential evapotranspiration (Pet), and snow depth in the KRB, ARB, YRB, and HRB.

in the ARB, YRB and HRB. For the TRB after 1961, there was a significant rise in temperatures and slight increase in precipitation. Rising temperatures have caused increased runoff from mountain regions, gave rise to snowmelt and glacier-melting (Lyu et al., 2015). In snow and ice melting dominated basin, like the YRB and HRB, runoff was more influenced by temperature than by precipitation. That is to say, in YRB and HRB, the occurrence of meteorological drought caused by low precipitation is less likely to lead to hydrological drought. Gao et al. (2010) found that, glacier meltwater contributed approximately 51.3% to the total runoff for the YRB during the 1961–2006 period, and it increased to about 63.3% after 2000 (Gao et al., 2010), while rainfall accounts for only 22% of the total runoff. The runoff recharge proportion from glacial meltwater in the HRB is up to about 57% (Li et al., 2018), and the runoff recharge proportions from precipitation is about 23% (Kan et al., 2018). In contrast, within precipitation and snowmelt dominated basins, like the KRB, runoff is influenced by both temperature and precipitation.

Based on the Chinese Glacier Inventory, the TRB in China has about 11665 glaciers, with the cumulative glacier area of about 19877.65 km^2 and an ice storage capacity of 2313.29 km^3. The basin possesses the largest number of glaciers and most glacier ice in China (Gao et al., 2010). Among the four source streams to the TRB, the YRB and HRB have the largest glacial area, accounting for about 54% of the glacial area of the entire TRB. Therefore, these two source streams have a relatively high percentage of glacier meltwater runoff. The glacial meltwater in the YRB, for example, accounting as high as 51.6%, and the change in glacier meltwater volume is mainly controlled by the fluctuation of glacier mass balance in the basin. Although precipitation in the four basins has been increasing in recent decades, the glacier mass balance in the basin has been decreasing due to increasing temperatures. A study by Gao et al. (2010) on the influence of glacial meltwater changes on runoff in the TRB from 1961 to 2006 found that the contribution of glacial retreat to the increase in runoff from the four source streams in the TRB was as high as 85.7%, much higher than the contribution of precipitation to runoff (Gao et al., 2010). Snowmelt can also alleviate drought to a certain extent, especially in spring. Taking KRB and ARB as an example, the contribution of snow melt to runoff in KRB and ARB is 49% and 22%, respectively (Chen et al., 2019a). The changes in runoff thus directly affect the Dd and Ds of hydrological drought and the variations of river runoff components in the TRB. When studying the mechanism of hydrological drought in this basin, drought cannot be predicted simply by the propagation transformation characteristics of meteorological droughts and hydrological droughts as in other basins; research requires a comprehensive consideration of relevant elements such as temperature, glacier mass balance, and snowpack, among other parameters (Duethmann et al., 2015, 2016).

The hydrological regimes in river headwater areas, especially in mountainous regions, is more sensitive to climate change and less sensitive to human activities. Rainfall runoff accounted for about 45%, 33%, 22%, and 31% in the KRB, ARB, YRB and HRB, respectively. These percentages of precipitation recharge are much lower than those of the wet and semi-humid areas in eastern China, such as the Yellow River, Luan River and Pearl River (Wang et al., 2019; Xu et al., 2019; Gu et al., 2020). These basins show a significant positive correlation between hydrological and meteorological droughts. In arid and semi-arid zones, river runoff responds to climatic change complexly (Li et al., 2017), and accordingly, the response of hydrological droughts to climate change factors is also complex and specific for a given region. In the study area, precipitation is no longer a key element affecting hydrological droughts. During periods when a meteorological drought occurs, low precipitation is often accompanied by high temperature, which in turn accelerates the melting of glacial snow, and for basins (Zhang et al., 2020) (e.g., the YRB) which are dominated by ice and snow meltwater recharge, it will instead provide more runoff and reduce the probability of a hydrological drought. On the contrary, precipitation is often accompanied by lower temperature within the study region, which inhibits the melting of snow and ice. It is at this time that the net inflow of snow and ice meltwater to rivers is low, and the probability of hydrological drought is higher. This also explains why there is a negative correlation between meteorological drought and hydrological drought in the glacier and snowmelt dominated YRB. Therefore, when formulating the water resources planning for the TRB, both precipitation and solid water reserves including glacier and snow should be considered under the influence of climate change.

5 Conclusions

In this paper, the 3-monthly scale SRI (SRI-3) and 3-monthly scale SPEI (SPEI-3) of four key upper catchments of the TRB of China, including the KRB, ARB, YRB, and HRB were calculated based on monthly-scale CRU gridded data set and runoff data collected at hydrological stations from 1961 to 2015, to investigate the spatiotemporal variability of meteorological and hydrological droughts in the four source streams. Two main hydrological drought event characteristics variables, Dd and Ds were defined based on Run theory, and the return periods were characterized by Copula functions. The propagation relationship of two types of droughts was then analyzed by correlation analysis and the wavelet method in the four basins. The following conclusions were drawn.

1) The optimal distribution functions of the standardized runoff indices of different measuring stations were different, and the GP, GEV, GM, and GP functions were selected to fit the runoff of each basin and calculate the standardized runoff indices according to the GOF test results.

2) From 1961 to 2015, the SRI-3 in all four basins showed an upward trend, with the YRB and HRB showing the most significant upward trend and greater interannual volatility; on the seasonal scale, the SRI-3 increased most significantly in winter, whereas it did not increase significantly in summer, although it also showed an upward trend. The trend of SPEI-3 showed a non-significant trend in the TRB, and this trend of SPEI-3 in the KRB and ARB was weak, with an increasing trend of 0.08/decade and 0.04/decade, respectively. This trend of SPEI-3 in the YRB and HRB was also weak, with negative trends of 0.06/decade and 0.05/decade, respectively.

3) The two-dimensional joint hydrological drought probabilities and return periods between Dd and Ds of the four basins were calculated. Results illustrate that the hydrological Dd and Ds of YRB and HRB were higher than those in KRB and ARB from 1961 to 2015. The joint drought probabilities of the four basins (the KRB, ARB, YRB and HRB) from 1961 to 2015 were 0.46, 0.46, 0.48, and 0.49, respectively, and the joint drought return periods were 4.86, 4.78, 3.72, and 5.57 years, respectively. With the increase of Dd and Ds, the corresponding drought return periods increased.

4) The correlation coefficients between SPEI and SRI were low in the four basins, and the maximum values of the correlation coefficients in the KRB, ARB, YRB and HRB were 0.52, 0.47, 0.25, and 0.21, respectively. The propagation time of meteorological droughts to hydrological droughts showed remarkable seasonal variations, being longer in spring and winter while shorter in summer and autumn. The results of the cross-wavelet analysis showed that the monthly SRI and SPEI series of each basin had different correlations in the time and frequency domains. Except for the YRB, which had a significant negative correlation, all other basins had significant positive correlations.

Acknowledgments The research is supported by the National Natural Science Foundation of China (Grant No. U1903208); Guangdong Foundation for Program of Science and Technology Research (Nos. 2020B1111530001 and 2019QN01L682), the GDAS Special Project of Science and Technology Development (Nos. 2020GDASYL-20200102013 and 2020GDASYL-20200301003). We thank LetPub for its linguistic assistance and scientific consultation during the preparation of this manuscript.

References

Ayantobo O O, Li Y, Song S, Javed T, Yao N (2018). Probabilistic modelling of drought events in China via 2-dimensional joint copula. J Hydrol (Amst), 559: 373–391

Bloomfield J P, Marchant B P (2013). Analysis of groundwater drought building on the standardized precipitation index approach. Hydrol Earth Syst Sci, 17(12): 4769–4787

Bushra N, Trepanier J C, Rohli R V (2019). Joint probability risk modelling of storm surge and cyclone wind along the coast of Bay of Bengal using a statistical copula. Int J Climatol, 39(11): 4206–4217

Chen H, Chen Y, Li W, Li Z (2019a). Quantifying the contributions of snow/glacier meltwater to river runoff in the Tianshan Mountains, Central Asia. Global Plan Chang, 174(MAR): 47–57

Chen X, Li F W, Li J Z, Feng P (2019b). Three-dimensional identification of hydrological drought and multivariate drought risk probability assessment in the Luanhe River Basin, China. Theor Appl Climatol, 137(3−4): 3055–3076

Chen Y, Li B, Li Z, Li W (2016a). Water resource formation and conversion and water security in arid region of northwest China. J Geogr Sci, 26(7): 939–952

Chen Y, Li W, Deng H, Fang G, Li Z (2016b). Corrigendum: changes in central Asia's water tower: past, present and future. Sci Rep, 6(1): 39364

Chen Y, Takeuchi K, Xu C, Chen Y, Xu Z (2006). Regional climate change and its effects on river runoff in the Tarim Basin, China. Hydrol Processes, 20(10): 2207–2216

Dodangeh E, Shahedi K, Shiau J T, Mirakbari M (2017). Spatial hydrological drought characteristics in Karkheh River Basin, southwest Iran using copulas. J Earth Syst Sci, 126(6): 80

Duethmann D, Menz C, Jiang T, Vorogushyn S (2016). Projections for headwater catchments of the Tarim River reveal glacier retreat and decreasing surface water availability but uncertainties are large. Environ Res Lett, 11(5): 054024

Duethmann D, Bolch T, Farinotti D, Kriegel D, Vorogushyn S, Merz B, Pieczonka T, Jiang T, Su B, Güntner A (2015). Attribution of streamflow trends in snow and glacier melt-dominated catchments of the Tarim River, central Asia. Water Resour Res, 51(6): 4727–4750

Fang G, Chen Y, Li Z (2018). Variation in agricultural water demand

and its attributions in the arid Tarim River Basin. J Agric Sci, 156(3): 301–311

Fernández B, Salas J D (1999). Return period and risk of hydrologic events. II: applications. J Hydrol Eng, 4(4): 308–316

Gao X, Ye B, Zhang S, Qiao C, Zhang X (2010). Glacier runoff variation and its influence on river runoff during 1961–2006 in the Tarim River Basin, China. Sci China Earth Sci, 53(6): 880–891

Gu L, Chen J, Yin J, Xu C Y, Chen H (2020). Drought hazard transferability from meteorological to hydrological propagation. J Hydrol (Amst), 585: 124761

Gudmundsson L, Boulange J, Do H X, Gosling S N, Grillakis M G, Koutroulis A G, Leonard M, Liu J, Müller Schmied H, Papadimitriou L, Pokhrel Y, Seneviratne S I, Satoh Y, Thiery W, Westra S, Zhang X, Zhao F (2021). Globally observed trends in mean and extreme river flow attributed to climate change. Science, 371(6534): 1159–1162

Hamed K H, Ramachandra Rao A (1998). A modified Mann-Kendall trend test for autocorrelated data. J Hydrol (Amst), 204(1−4): 182–196

Hirsch R M, Slack J R (1984). A nonparametric trend test for seasonal data with serial dependence. Water Resour Res, 20(6): 727–732

Huang S, Li P, Huang Q, Leng G, Hou B, Ma L (2017). The propagation from meteorological to hydrological drought and its potential influence factors. J Hydrol (Amst), 547: 184–195

Jiao Y, Yuan X (2019). More severe hydrological drought events emerge at different warming levels over the Wudinghe watershed in northern China. Hydrol Earth Syst Sci, 23(1): 621–635

Kan B, Su F, Xu B, Xie Y, Li J, Zhang H (2018). Generation of high mountain precipitation and temperature data for a quantitative assessment of flow regime in the Upper Shache Basin in the Karakoram. J Geophys Res D Atmospheres, 123(16): 8462–8486

Kao S, Govindaraju R S (2010). A copula-based joint deficit index for droughts. J Hydrol (Amst), 380(1−2): 121–134

Li B, Chen Y, Chipman J W, Shi X, Chen Z (2018). Why does the runoff in Hotan River show a slight decreased trend in northwestern China? Atmos Sci Lett, 19(1): e800

Li J, Zhou S, Hu R (2016). Hydrological drought class transition using SPI and SRI time series by loglinear regression. Water Resour Manage, 30(2): 669–684

Li Q, He P, He Y, Han X, Zeng T, Lu G, Wang H (2020). Investigation to the relation between meteorological drought and hydrological drought in the upper Shaying River Basin using wavelet analysis. Atmos Res, 234: 104743

Li Z, Chen Y, Fang G, Li Y (2017). Multivariate assessment and attribution of droughts in central Asia. Sci Rep, 7(1): 1316

Lyu J, Shen B, Li H (2015). Dynamics of major hydro-climatic variables in the headwater catchment of the Tarim River Basin, Xinjiang, China. Quat Int, 380−381: 143−148

Ma F, Luo L, Ye A, Duan Q (2019). Drought characteristics and propagation in the semiarid Heihe River Basin in northwestern China. J Hydrometeorol, 20(1): 59–77

Mercado V D, Perez G C, Solomatine D, Van Lanen H J (2016). Spatio-temporal analysis of hydrological drought at catchment scale using a spatially-distributed hydrological model. Procedia Eng, 154: 738–744

Mirabbasi R, Fakheri-Fard A, Dinpashoh Y (2011). Bivariate drought frequency analysis using the copula method. Theor Appl Climatol, 108(1−2): 191–206

Oloruntade A J, Mohammad T A, Ghazali A H, Wayayok A (2017). Analysis of meteorological and hydrological droughts in the Niger-South Basin, Nigeria. Global Planet Change, 155: 225–233

Peng J, Chen S, Dong P (2010). Temporal variation of sediment load in the Yellow River Basin, China, and its impacts on the lower reaches and the river delta. Catena, 83(2−3): 135–147

Serinaldi F, Bonaccorso B, Cancelliere A, Grimaldi S (2009). Probabilistic characterization of drought properties through copulas. Phys Chem Earth Parts ABC, 34(10−12): 596–605

Shukla S, Wood A W (2008). Use of a standardized runoff index for characterizing hydrologic drought. Geophys Res Lett, 35(2): L02405

Svensson C, Hannaford J, Prosdocimi I (2017). Statistical distributions for monthly aggregations of precipitation and streamflow in drought indicator applications. Water Resour Res, 53(2): 999–1018

Tak S, Keshari A K (2020). Investigating mass balance of Parvati glacier in Himalaya using satellite imagery based model. Sci Rep, 10(1): 12211

Telesca L, Lovallo M, Lopez-Moreno I, Vicente-Serrano S (2012). Investigation of scaling properties in monthly streamflow and standardized streamflow index (SSI) time series in the Ebro basin (Spain). Physica A, 391(4): 1662–1678

Tirivarombo S, Osupile D, Eliasson P (2018). Drought monitoring and analysis: standardised precipitation evapotranspiration index (SPEI) and standardised precipitation index (SPI). Phys Chem Earth, 106: 1–10

Torrence C, Compo G P (1998). A practical guide to wavelet analysis. Bull Am Meteorol Soc, 79(1): 61–78

Torrence C, Webster P J (1999). Interdecadal changes in the ENSO–monsoon system. J Clim, 12(8): 2679–2690

Trenberth K E, Fasullo J T (2013). An apparent hiatus in global warming? Earths Futur, 1(1): 19−32

Vicente-Serrano S M, López-Moreno J I, Beguería S, Lorenzo-Lacruz J, Azorin-Molina C, Morán-Tejeda E (2012). Accurate computation of a streamflow drought index. J Hydrol Eng, 17(2): 318–332

Vicente-Serrano S M, Quiring S M, Peña-Gallardo M, Yuan S, Domínguez-Castro F (2020). A review of environmental droughts: Increased risk under global warming? Earth Sci Rev, 201: 102953

Wang A, Wang Y, Su B, Kundzewicz Z W, Tao H, Wen S, Qin J, Gong Y, Jiang T (2020a). Comparison of changing population exposure to droughts in river basins of the Tarim and the Indus. Earth Future, 8: e2019EF001448

Wang F, Wang Z, Yang H, Di D, Zhao Y, Liang Q, Hussain Z (2020b). Comprehensive evaluation of hydrological drought and its relationships with meteorological drought in the Yellow River Basin, China. J Hydrol (Amst), 584: 124751

Wang H, Chen Z, Chen Y, Pan Y, Feng R (2019). Identification of the space-time variability of hydrological drought in the arid region of northwestern China. Water, 11(5): 1051

Williams A P, Seager R, Abatzoglou J T, Cook B I, Smerdon J E, Cook

E R (2015). Contribution of anthropogenic warming to California drought during 2012–2014. Geophys Res Lett, 42(16): 6819–6828

Wu R, Zhang J, Bao Y, Guo E (2019). Run theory and Copula-based drought risk analysis for Songnen Grassland in northeastern China. Sustainability, 11(21): 6032

Xiang Y, Wang Y, Chen Y, Bai Y, Zhang L, Zhang Q (2020). Hydrological drought risk assessment using a multidimensional Copula function approach in arid inland basins, China. Water, 12(7): 1888

Xu Y, Zhang X, Wang X, Hao Z, Singh V P, Hao F (2019). Propagation from meteorological drought to hydrological drought under the impact of human activities: a case study in northern China. J Hydrol (Amst), 579: 124147

Zhang A, Zhang C, Fu G, Wang B, Bao Z, Zheng H (2012). Assessments of impacts of climate change and human activities on runoff with SWAT for the Huifa River Basin, northeast China. Water Resour Manage, 26(8): 2199–2217

Zhang L, Singh V P (2007). Gumbel–Hougaard Copula for trivariate rainfall frequency analysis. J Hydrol Eng, 12(4): 409–419

Zhang Q, Chen Y, Li Z, Fang G, Xiang Y, Li Y, Ji H (2020). Recent changes in water discharge in snow and glacier melt-dominated rivers in the Tienshan Mountains, Central Asia. Remote Sens, 12(17): 2704

Zhong F, Cheng Q, Wang P (2020). Meteorological drought, hydrological drought, and NDVI in the Heihe River Basin, northwest China: evolution and propagation. Adv Meteorol, 2020: 1–26

Zhou Z, Shi H, Fu Q, Ding Y, Li T, Wang Y, Liu S (2021). Characteristics of propagation from meteorological drought to hydrological drought in the Pearl River Basin. J Geophys Res D Atmospheres, 126(4): e2020JD033959

AUTHOR BIOGRAPHIES

Yanyun Xiang received her D. Sc. Degree in State Key Laboratory of Desert and Oasis Ecology, Xinjiang Institute of Ecology and Geography, Chinese Academy of Sciences. She is specialized in Hydrological drought, hydrology and water resource in arid area.

Yi Wang is a professor in State Key Laboratory of Desert and Oasis Ecology, Xinjiang Institute of Ecology and Geography, Chinese Academy of Sciences. She is specialized in hydrological process research; mitigation and prevention of related water disasters under the influence of climate change.

Yaning Chen is a professor in State Key Laboratory of Desert and Oasis Ecology, Xinjiang Institute of Ecology and Geography, Chinese Academy of Sciences. He is specialized in hydrology and water resources in arid area; eco-hydrological process; climate change in arid region; resource development and environmental improvement.

Qifei Zhang received his D.Sc. Degree in State Key Laboratory of Desert and Oasis Ecology, Xinjiang Institute of Ecology and Geography, Chinese Academy of Sciences. He is specialized in glacier change and water resources.

Hongwei Li is a graduate student in State Key Laboratory of Desert and Oasis Ecology, Xinjiang Institute of Ecology and Geography, Chinese Academy of Sciences. His current research includes climate change and meteorological drought in global.